

Plasma characterization with terahertz time-domain measurements

S. P. Jamison^{a)}

Department of Physics and Applied Physics, University of Strathclyde, Glasgow, G4 0NG, United Kingdom

Jingling Shen

Department of Physics, Capital Normal University, Beijing, China

D. R. Jones, R. C. Issac, B. Ersfeld, D. Clark, and D. A. Jaroszynski

Department of Physics and Applied Physics, University of Strathclyde, Glasgow, G4 0NG, United Kingdom

(Received 9 September 2002; accepted 21 January 2003)

Terahertz time-domain spectral techniques are applied to the characterization of a He discharge plasma. Electro-optically sampling of the electric field of a quasi-unipolar terahertz pulse transmitted through the plasma has allowed both the real and imaginary parts of the plasma permittivity to be simultaneously measured over a large spectral range. The plasma density and the collisional frequency are determined within a 30 ps duration measurement window. An anomalously high collisional frequency has been measured. © 2003 American Institute of Physics.

[DOI: 10.1063/1.1560564]

Microwave techniques are well established as important diagnostic tools for characterizing low-density plasma.¹ The advent of the laser has extended these interferometric techniques to plasmas with densities as high as 10^{19} cm^{-3} .² Both microwave and laser techniques suffer from the disadvantage that they require the use of a number of sources of different frequencies to unambiguously determine the phase change induced by the real part of the refractive index, n , of the extended plasma. In this article, we present techniques based on terahertz time-domain spectroscopy (THz-TDS), which provide a powerful time resolved method for fully characterizing gaseous plasma over a wide range of densities. This method should find application in the characterization and monitoring of industrial plasma, tokomaks, wakefield accelerators, radiation sources based laser-plasma interactions, and conventional gas lasers plasma.

The plasma frequency, $\omega_p = \sqrt{n_e e^2 / \epsilon_0 m_e}$, is the natural resonant frequency of a plasma where n_e is the electron number density and m_e is the electron mass. In the absence of magnetic fields, the propagation and attenuation constants, κ and α , of the wave in the medium are given by $k = \text{Re}\{\epsilon^{1/2}\}\omega/c$ and $\alpha = \text{Im}\{\epsilon^{1/2}\}\omega/c$, respectively, which are a function of the complex dielectric constant,

$$\epsilon = \left(1 - \frac{\omega_p^2}{\omega^2 + \nu^2}\right) - i \left(\frac{\nu}{\omega} \frac{\omega_p^2}{\omega^2 + \nu^2}\right), \quad (1)$$

where ν is the average momentum transfer collision rate. Thus, by measuring the absorption and phase delay of a wave traveling through a plasma, we are able to deduce the plasma density and the collisional frequency. The techniques of THz-TDS have been extensively applied to semiconductor plasma characterization,^{3,4} and have recently been employed in subpicosecond time resolved determinations of semiconductor carrier dynamics.⁵ However, these techniques have

not previously been demonstrated for gaseous plasma, which have plasma frequency and collisional rates orders of magnitude smaller than those in a semiconductor plasma.

In the techniques described here, an ultrafast subpicosecond duration, broadband source of coherent far-infrared (THz) radiation is used to measure the density of a He discharge plasma over a range of $n_e \sim 10^{11} \text{ cm}^{-3} - 10^{13} \text{ cm}^{-3}$ and a typical collisional frequency of $\sim 10^{11} \text{ s}^{-1}$. The plasma properties are measured with a time resolution of 30 ps, corresponding to the sampling window. The spectrum of the THz pulse contains frequencies close to the plasma frequency, which enables much lower plasma densities to be measured than possible using interferometric techniques based on mid-IR to visible wavelength lasers.² The large absorption in the THz frequency range also makes these THz-time-domain methods a very direct and practical method of measuring collisional properties of the plasma.

In the experiments described here, a biased large area GaAs wafer Auston switch⁶ is used to generate a quasi-unipolar subpicosecond THz radiation pulse. The electric field of the free space THz pulse transmitted through the plasma is sampled using electro-optic detection in ZnTe.⁷ A Ti:Sapphire laser provides $\sim 1 \text{ mJ}$, 800 nm, 80 fs long pulses for initiating the THz emission from the GaAs emitter, and sampling the THz pulse in a 1 mm thick (110) ZnTe crystal.

A uniform plasma was created in a 15 cm long 2 cm diameter tube filled with 24 mbar of helium. A transient electrical discharge was provided by a 1 kHz, 6 kV, 50 ns rise time solid-state high voltage pulse power supply, which was synchronized with the Ti:Sapphire laser. A variable delay between the laser and power supply allowed the plasma to be measured at different times thus enabling the properties to be sampled over the $\sim 300 \text{ ns}$ discharge current risetime. A $f/10$ focusing system was used to pass the probe THz pulse through the plasma tube and fused silica windows.

Standard THz-TDS techniques are used to make subpicosecond resolution measurements of the phase shifts and

^{a)} Author to whom correspondence should be addressed; electronic mail: steven.jamison@strath.ac.uk

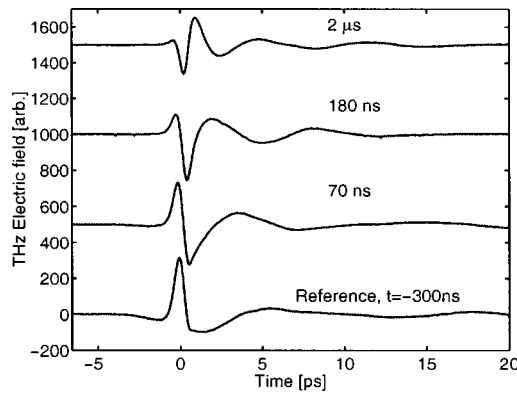


FIG. 1. THz pulse wave forms for various delays with respect to the peak of the tube voltage, which occurs at $t=50$ ns.

amplitude changes experienced by the THz probe on transmission through the plasma over the full spectral bandwidth available. The measurement of the time domain electric field is made over a 30 ps window, allowing the frequency dependence of the absorption coefficients and refractive indices to be determined with a spectral resolution of 40 GHz.⁸

Figure 1 shows the THz probe pulse after propagation through the plasma region measured for various time delays with respect to the initial rise of the discharge voltage pulse. A THz reference pulse is obtained from a measurement with the THz pulse preceding the discharge. The first observable changes in the transmitted THz pulse shape occur 20 ns before the peak of the tube voltage and large distortion is obvious 40 ns later due to the increase in plasma density and collisional frequency.

The spectrally resolved dispersion and absorption of the THz pulse, over the full bandwidth, is calculated from the (complex) field spectrum $\tilde{E}(\omega)$, which is obtained from the Fourier transform of the time resolved measurement of the electric field $E(t)$. For a longitudinally uniform plasma, the difference between the reference and plasma spectra is due to the change in the propagation and absorption coefficients,

$$\tilde{E}_{\text{plas}}(\omega) = T\tilde{E}_{\text{ref}}(\omega)\exp(i(k_{\text{plas}} - k_0)L)\exp(-\alpha L), \quad (2)$$

where L is length of plasma traversed by the THz pulse, k_0 is the propagation wavenumber in the absence of plasma, α is the absorption coefficient, and T is the Fresnel transmission coefficient of the boundaries.

The dispersion of the THz pulse is inferred from the phase changes and compared with the calculated values. While, in principle, dispersion and absorption in plasma depend on both the electron density and the collisional frequency, the dispersion depends strongly only on electron density for frequencies greater than the plasma frequency. Thus for ν , $\omega_p < \omega$, and $\nu \approx \omega_p$, the plasma propagation coefficient can be approximated as

$$k_{\text{plas}}^2 \approx \frac{\omega^2}{c^2} \left(1 - \frac{\omega_p^2}{\omega^2 + \nu^2} \right) \left[1 + \frac{1}{4} \left(\frac{\omega_p^2}{(\omega^2 + \nu^2 - \omega_p^2)} \frac{\nu}{\omega} \right)^2 \right], \quad (3)$$

from which it follows that the frequency dependent phase change will be

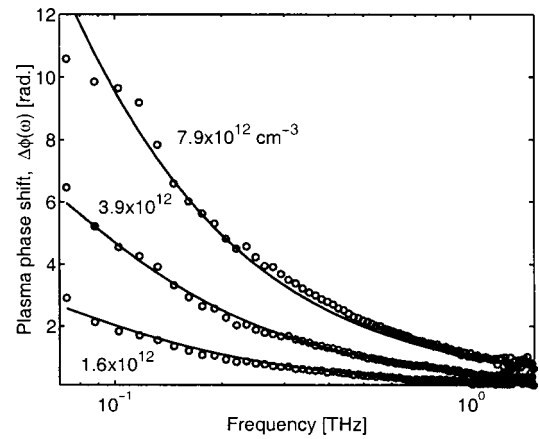


FIG. 2. Measured and calculated plasma induced phase shifts for different plasma densities for the THz wave forms of Fig. 1. Plasma density increases with time delay between the tube voltage peak and THz probe.

$$\Delta\Phi = \arg\{\tilde{E}_{\text{plas}}(\omega)\} - \arg\{\tilde{E}_{\text{ref}}(\omega)\} \approx \frac{\omega L}{c} \left[\left(1 - \frac{\omega_p^2}{\omega^2 + \nu^2} \right)^{1/2} - 1 \right]. \quad (4)$$

The $m2\pi$ ambiguities in $\Delta\Phi(\omega)$ are removed by ensuring continuity over the full measured frequency range. A remaining phase ambiguity is resolved from the high-frequency limit, $\omega \gg \omega_p$, for which the measured phase change tends toward zero. Figure 2 shows the measured plasma induced phase change at different times in the evolution of the plasma density. As the frequency approaches the plasma frequency $\omega \rightarrow \omega_p^+$, the gradient of the phase $\partial\Delta\Phi/\partial\omega$ becomes sufficiently large for a 2π phase change to occur within the spectral resolution of the measurement, at which point continuity of the phase fails. This provides a lower-frequency limit for the phase measurements. The restriction of phase jumps to less than π within the spectral resolution $\delta\omega$ requires $(\partial\Delta\Phi/\partial\omega)\delta\omega \sim L\omega_p^2\delta\omega/2c\omega^2 \leq \pi$. For the measurements presented here, the spectral resolution is $\delta\omega = 0.04$ THz, thus the low-frequency limit for the unambiguous determination of the phase for a plasma density of 10^{13} cm^{-3} is 0.13 THz, as can be seen in Fig. 2.

The momentum transfer collision rate is obtained from the frequency dependent absorption of the THz radiation. From a series expansion of the absorption coefficient,

$$\alpha^2 \approx \frac{\omega^2}{4c^2} \left(1 - \frac{\omega_p^2}{\omega^2 + \nu^2} \right) \left[\frac{\omega_p^2}{(\omega^2 + \nu^2 - \omega_p^2)} \frac{\nu}{\omega} \right]^2, \quad (5)$$

it is clear that absorption depends on both the electron density and the collisional frequency ($\omega_p^2\nu \sim n_e\nu$). To separate these parameters, the electron density is first determined from the phase change and then the collision rate is determined from transmission spectra using the measured values of the plasma density. This procedure is iterated to obtain convergence for consistent density and collision rates, usually within two or three iterations. The complex permittivity of Eq. (1), rather than the approximations given herein, is used in the iteration. For the limiting case of sharp discontinuous boundaries, the transmission coefficient T gives rise

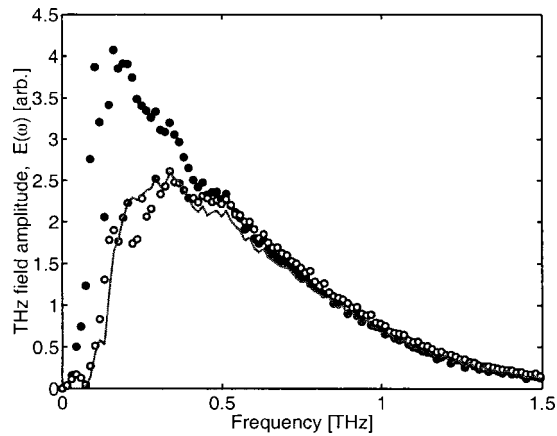


FIG. 3. THz spectral amplitude with and without plasma (empty and filled circles, respectively), for $t=2\ \mu\text{s}$ wave forms of Fig. 1. The calculated transmission spectrum (solid line) corresponds to an electron density and collisional frequency of $n_e=7.9\times 10^{12}\text{ cm}^{-3}$ and $\nu=1.6\times 10^{11}\text{ s}^{-1}$, respectively.

to a less than 1% change in the collision frequency, and can therefore be taken as $T=1$ over the frequency range considered here. It is noted that, in similarity to interferometric measurements the determined plasma density is linearly dependent on the assumed plasma length,² however the measured collision frequency is almost totally independent of the plasma extent. This independence is a consequence of the approximate $Ln_e\nu$ dependence of the transmission losses. Figure 3 shows an example of the measured and calculated transmission spectra where the calculated spectrum is obtained from the measured reference spectra by $|E(\omega)_{\text{calc}}| = |E(\omega)_{\text{ref}}|\exp(-\alpha L)$.

The evolution of electron density and collision rate obtained for the helium discharge are presented in Fig. 4. An electron density in the range 10^{11} cm^{-3} – 10^{13} cm^{-3} is measured and two distinct regions are observed: A rapid increase in density over the first 50 ns followed by a slower increase in density over the following $1\ \mu\text{s}$. The collision frequency is observed to increase in a similar way up to $1\ \mu\text{s}$ to reach a maximum of $\nu=3\times 10^{11}\text{ s}^{-1}$ at $1\ \mu\text{s}$ and then decreases slowly as the plasma cools and recombines over the next millisecond. At the measured plasma densities, the collisional frequency is dominated by electron–neutral collisions. Previous studies of microwave excited He discharges give an electron temperature of $\sim 5\text{ eV}$.¹⁰ From the e^- –He collisional cross sections,⁹ a collisional frequency of $\sim 6\times 10^{10}\text{ s}^{-1}$ is expected. However, these estimates differ from the largest collisional frequency measured here by a factor of 5.

Anomalously high absorption can arise from nonlinear

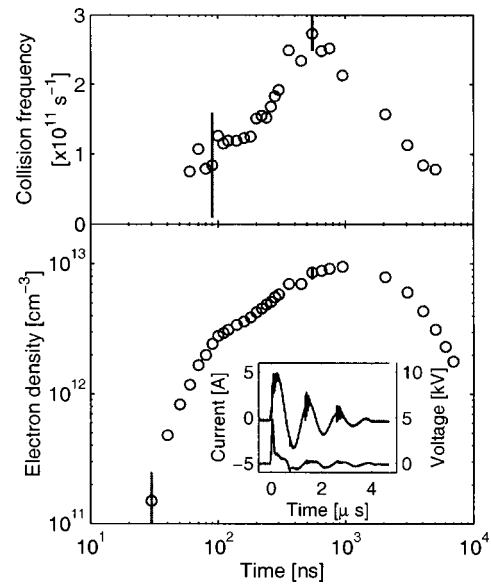


FIG. 4. The time dependence of the plasma electron density and collisional momentum transfer rate determined from the THz-TDS measurements. The inset shows the evolution of the discharge tube current and voltage. Error bars are estimated for representative data.

effects due to the high electric field of an electromagnetic probe accelerating the electrons to velocities comparable to thermal velocities.¹¹ However, this has been discounted by measurements of the absorption using a THz electric-field amplitude reduced by a factor of ~ 3 which yielded the same collisional frequencies.

In summary, THz-TDS methods have been used to measure properties of a He discharge plasma such as density and collisional frequency. However, the origin of the anomalously high measured collisional frequency will need to be found before the method can be applied to determining the temperature of the plasma.

¹M. A. Heald and C. B. Wharton, *Plasma Diagnostics with Microwaves* (Wiley, New York, 1965).

²D. J. Spence, P. D. S. Burnett, and S. M. Hooker, *Opt. Lett.* **24**, 993 (1999).

³M. Van Exter and D. Grischkowsky, *Phys. Rev. B* **41**, 12140 (1990).

⁴M. C. Beard, G. M. Turner, and C. A. Schmuttenmaer, *Phys. Rev. B* **62**, 15764 (2000).

⁵A. Leitenstorfer, R. Huber, F. Tauser, A. Brodschelm, M. Bichler, and G. Abstreiter, *Physica B* **314**, 248 (2002); R. Huber, F. Tauser, A. Brodschelm, M. Bichler, G. Abstreiter, and A. Leitenstorfer, *Nature (London)* **414**, 286 (2001).

⁶D. You, R. R. Jones, P. H. Bucksbaum, and D. R. Dykaar, *Opt. Lett.* **18**, 290 (1993).

⁷Q. Wu and X.-C. Zhang, *Appl. Phys. Lett.* **71**, 1285 (1997).

⁸R. A. Cheville and D. Grischkowsky, *J. Opt. Soc. Am. B* **16**, 317 (1999).

⁹L. S. Frost and A. V. Phelps, *Phys. Rev. A* **136**, 1538 (1964).

¹⁰M. R. Talukder, D. Korzec, and M. Kando, *J. Appl. Phys.* **91**, 9529 (2002).

¹¹V. P. Silin, *Sov. Phys. JETP* **20**, 1510 (1965); B. Ersfeld and A. R. Bell, *Phys. Plasmas* **7**, 1001 (2000).